ISA Transactions 53 (2014) 85–96

Contents lists available at ScienceDirect

ISA Transactions

journal homepage: www.elsevier.com/locate/isatrans

Research Article

PID controller auto-tuning based on process step response and damping optimum criterion

Danijel Pavković [a,*], Siniša Polak [b], Davor Zorc [a,1]

[a] Faculty of Mechanical Engineering and Naval Architecture, University of Zagreb, I. Lučića 5, HR-10000 Zagreb, Croatia
[b] INA-Oil Industry d.d. – Sisak Oil Refinery, Ante Kovačića 1, HR-44000 Sisak, Croatia

ARTICLE INFO

Article history:
Received 2 November 2012
Received in revised form
12 March 2013
Accepted 19 August 2013
Available online 12 September 2013
This paper was recommended for publication by Dr. K.A. Hoo

Keywords:
PID controller
PTn process model
Damping optimum criterion
Identification
Auto-tuning control

ABSTRACT

This paper presents a novel method of PID controller tuning suitable for higher-order aperiodic processes and aimed at step response-based auto-tuning applications. The PID controller tuning is based on the identification of so-called *n*-th order lag (PTn) process model and application of damping optimum criterion, thus facilitating straightforward algebraic rules for the adjustment of both the closed-loop response speed and damping. The PTn model identification is based on the process step response, wherein the PTn model parameters are evaluated in a novel manner from the process step response equivalent dead-time and lag time constant. The effectiveness of the proposed PTn model parameter estimation procedure and the related damping optimum-based PID controller auto-tuning have been verified by means of extensive computer simulations.

1. Introduction

Many industrial processes such as heat and fluid flow processes are characterized by slow aperiodic dynamics (lag behavior) and dead-time (transport delay), which are frequently modeled by a control-oriented first-order plus dead-time (FOPDT) process model [1,2], and are in a majority of cases still controlled by Proportional-Integral-Derivative (PID) controllers [3–5]. Accordingly, the PID controller auto-tuning still remains an interesting and propulsive R&D field (see [6] and references therein), which has resulted in numerous PID controller auto-tuning patents and commercial controller units over the last several decades [7]. Among the patented and implemented PID adaptation approaches the so-called analytical formula methods, typically based on process open-loop (input step) or closed-loop (limit-cycle) excitation test are usually preferred over more complex tuning methods, such as those based on heuristic rules, artificial intelligence and numerical optimization approaches. In latter cases the closed-loop behavior is typically monitored with the PID controller turned on, and PID controller adaptation is performed in real-time without applying a dedicated test signal [8].

The conventional formula-based tuning methods, such as the Ziegler–Nichols (ZN) tuning rules, even though still used in practical applications due to their simplicity, may result in a relatively large closed-loop step response overshoot and related weak response damping [9,10]. The closed-loop damping issues have been traditionally addressed by using the Chien–Hrones–Reswick (CHR) ZN rule modification based on the time-domain FOPDT process model identification, while the so-called Kappa-Tau method has been used for frequency response-based (i.e. ultimate point finding) auto-tuning [11,12]. Some of the more recent efforts at ZN-rule improvement have included controller parameters numerical optimization for a wide range of FOPDT process model parameters variations [5], and on-line adaptation of the PID controller proportional gain [10].

In order to further improve the PID controller performance compared to the above traditional tuning formulas, a wide range of process excitation-based auto-tuning approaches has been proposed in the literature over the last decade or so, which may be categorized as

- *Frequency response-based approaches* aimed at (i) improved gain and phase margin estimation [13–15], (ii) process model identification based on closed-loop relay experiment in combination with internal model control (IMC) based controller tuning for improved control-loop load disturbance rejection [16], (iii) using a more general case of binary noise signal for the process model frequency characteristic identification and loop-shaping-based controller tuning for robust behavior [17], (iv) use of Bode's integrals for improved closed-loop system robustness [18], and (v) relay experiment with cascaded

* Corresponding author. Tel.: +385 1 6168 325; fax: +385 1 6168 351.
E-mail addresses: danijel.pavkovic@fsb.hr (D. Pavković), Sinisa.Polak@ina.hr (S. Polak), davor.zorc@fsb.hr (D. Zorc).
[1] Tel.: +385 1 6168 436; fax: +385 1 6168 351.

0019-0578/$ - see front matter © 2013 ISA. Published by Elsevier Ltd. All rights reserved.
http://dx.doi.org/10.1016/j.isatra.2013.08.011

PI controller for load disturbance compensation and filtering effect during process model identification [19]. For a rather comprehensive review of relay-feedback frequency-domain auto-tuning methods the reader is also referred to [20].

- *Time response approaches* based on (i) process output multiple integration and regression analysis in order to find the parameters of a second-order plus dead-time (SOPDT) process model [21], (ii) multiple process step response integration to find a general linear process model [22–24] combined with the utilization of the so-called magnitude optimum criterion in order to achieve well-damped closed-loop response, and (iii) step-response identification of FOPDT model combined with IMC tuning approach [25,26], or a robust loop-shaping controller design (the so-called AMIGO method) [26,27].
- *Combined approaches* wherein the time-domain and frequency-domain process model identification is used, such as the combined relay experiment+step response identification of a FOPDT process model [28], or a random signal-based process excitation and SOPDT process model parameters estimation and controller tuning based on zero-pole conditioning (canceling) [29].

However, in most of the above cases the PID controller tuning was based on the relatively simple FOPDT (or SOPDT) process model approximation with first-order Taylor or Padé dead-time approximations used for the purpose of PID controller design, which may not be accurate in the presence of more pronounced higher-order process dynamics. In order to capture the higher-order dynamics, while simultaneously having a relatively simple dead-time-free process model formulation, an *n*-th order lag process model (the so-called PTn model) can conveniently be used, wherein analytical relationships between the PTn model and FOPDT model parameters are typically given through the equivalence of the process model step response flexion tangent (the so-called Strejc method) [30,31]. By utilizing the PTn process model as the basis for the control system design in [32], straightforward analytical expressions have been derived for the PID controller parameters based on the magnitude optimum criterion (see e.g. [33] and references therein). The PTn model parameters have been identified in [32] by using the so-called moment method (see e.g. [30]), implemented through multiple time-weighted integrations of the process output, thus avoiding the estimation of the process step response flexion tangent slope (and related measurement noise issues). Since the main advantage of the magnitude optimum criterion is that it can assure a well-damped (over-damped) closed-loop system response, this approach has also been pursued for a wider class of linear process models in [22]. Further refinements of the tuning method from [22] have included a filtering term added to the PID controller transfer function to facilitate relatively straightforward closed-loop response speed (response time) tuning [23], and extending the PID controller with a reference pre-filtering or weighting action to facilitate separate closed-loop system tuning with respect to reference and external disturbance [24].

Still, the aforementioned magnitude optimum-based PID controller auto-tuning does not provide a straightforward way of closed-loop damping adjustment, while the repetitive integration of process output may result in an increased computational burden of the PID controller auto-tuning algorithm, especially if application on a relatively low-cost industrial controller is considered. Hence, a more flexible pole-placement-like tuning method, as well as a simpler process step response-based auto-tuning experiment (e.g. based on a single integration of process step response) would result in a more accommodating and less-demanding PID auto-tuner realization. To this end, this paper proposes a PID controller tuning approach based on the so-called damping optimum criterion [34,35] in combination with the PTn process model formulation, which facilitates an analytical and straightforward way of adjusting both the closed-loop response damping and response speed with respect to process dynamics. The estimation of PTn process model parameters is based herein on the single integration of the process step response in order to find the parameters of the basic FOPDT process model. The simpler FOPDT model is then related to the equivalent dead-time-free PTn model by using a higher-order Taylor expansion of the dead-time (pure delay) dynamic term via simple analytical expressions. The proposed PID controller tuning, the FOPDT and PTn process model identification procedures and the resulting PID controller auto-tuning algorithm is verified by means of extensive computer simulations.

The paper is organized as follows. Section 2 presents the analytical control system design procedure based on the damping optimum criterion and the compact PTn aperiodic process model, and illustrates the effectiveness of resulting closed-loop damping and response speed tuning method. These results are also accompanied by the analysis of the closed-loop robustness with respect to modeling uncertainties. The identification of PTn process model, based on a single integration of the process output is described in Section 3. The proposed identification procedure and the related PID controller auto-tuning are thoroughly tested in Section 4 by means of simulations. Concluding remarks are given in Section 5.

2. Control system design

This section presents the damping optimum criterion-based tuning of the PID controller for the process model with aperiodic step response dynamics, including the compact-form PTn process model. The effectiveness of the proposed PID controller tuning procedure, including the closed-loop damping tuning is illustrated by means of simulations.

2.1. Control system structure

The structure of the linear control system comprising a modified PID feedback controller (the so-called I+PD controller, [41]) is shown in Fig. 1. In comparison with the traditional PID controller where the proportional (P), integral (I), and derivative (D) terms are placed into the path of the control error *e*, the proportional and derivative terms of the modified PID controller act upon the measured process output *y* only (Fig. 1). By opting to use the modified PID controller structure which does not introduce additional controller zeros in the closed-loop transfer function, the desired closed-loop system behavior can be achieved with respect to the external disturbance *w*, while also avoiding the potentially excessive control effort related to sudden reference y_R changes or "noisy" reference. Since the proposed control system design does not introduce additional closed-loop zeros due to controller P+D action, the proposed approach also results in relatively simple

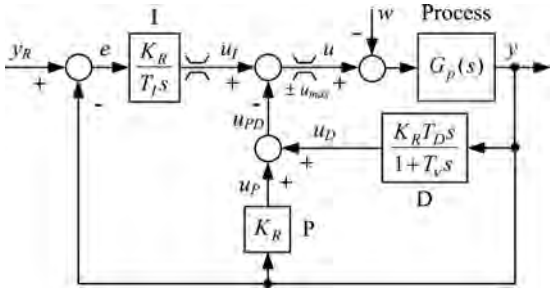

Fig. 1. Block diagram of control system with modified PID controller.

and straightforward PID controller tuning rules (see Section 2.2). Should the traditional PID controller structure be preferred, or the reference and disturbance behavior of the closed-loop system be tuned independently, somewhat more complex (two-step) tuning approaches may be required, such as those presented in Refs. [24,36], wherein the magnitude optimum-based tuning has been proposed to separately tune the closed-loop system response with respect to reference.

Note that in order to avoid relatively large step response overshoots in the large-signal operating mode (so-called integrator windup problem), the controller integral term should be saturated when controller output saturation is performed (Fig. 1), e.g. by using the so-called reset-integrator method [37].

It is assumed that the process is characterized by relatively slow aperiodic dynamics (no step response overshoot or transient oscillations), which can be approximated by the n-th order aperiodic process model with a single time constant T_p (the so-called PTn model) [30–32], given in the following compact transfer function form:

$$G_p(s)=\frac{y(s)}{u(s)}=\frac{K_p}{(1+T_p s)^n}=\frac{K_p}{1+a_1 s+a_2 s^2+\cdots a_n s^n}, \tag{1}$$

where K_p is the PTn model gain, $n\geq 2$ is the process order, and the parameters of the process model characteristic polynomial a_m ($m=1\ldots n$) are given by

$$a_m=\binom{n}{m}T_p^m=\frac{n!}{m!(n-m)!}T_p^m. \tag{2}$$

2.2. PID controller tuning

The PID controller tuning procedure is based on the damping optimum (or double ratios) criterion [34,35]. This is a pole-placement-like analytical method of design of linear continuous-time closed-loop systems with a full or reduced-order controller, which results in straightforward analytical relations between the controller parameters, the parameters of the process model, and desired level of response damping via characteristic design-specific parameters. Even though somewhat less well known than the magnitude optimum criterion [33], the damping optimum criterion has found application in those control systems where the closed-loop damping needs to be tuned in a precise and straightforward manner (e.g. in electrical servodrives with emphasized transmission compliance effects, see [38–40]).

The tuning procedure starts with the transfer function of the closed-loop control system in Fig. 1 assuming idealized PID controller (typically, the derivative filter time constant $T_\nu \ll T_D$, so it may be neglected):

$$G_c(s)=\frac{y(s)}{y_R(s)}=1/\left(1+\frac{(1+K_R K_p)T_I s}{K_R K_p}+\frac{(K_R K_p T_D+a_1)T_I s^2}{K_R K_p}+\frac{a_2 T_I s^3}{K_R K_p}+\frac{a_3 T_I s^4}{K_R K_p}+\cdots+\frac{a_n T_I s^{n+1}}{K_R K_p}\right). \tag{3}$$

The characteristic polynomial of the closed-loop system (3) can be rewritten in terms of the damping optimum criterion in the following form:

$$G_c(s)=\frac{1}{A_c(s)}=\frac{1}{1+T_e s+D_2 T_e^2 s^2+D_3 D_2^2 T_e^3 s^3\cdots+D_l D_{l-1}^2\cdot\cdots D_2^{l-1}T_e^l s^l}, \tag{4}$$

where T_e is the equivalent time constant of the overall closed-loop system, D_2, D_3, …, D_l are the so-called damping optimum characteristic ratios, and l is the closed-loop system order ($l=n+1$ in the case of PID controller, cf. (3)).

When all characteristic ratios are set to the so-called "optimal" values $D_2=D_3=\ldots=D_l=0.5$ (e.g. by applying a full-order controller),

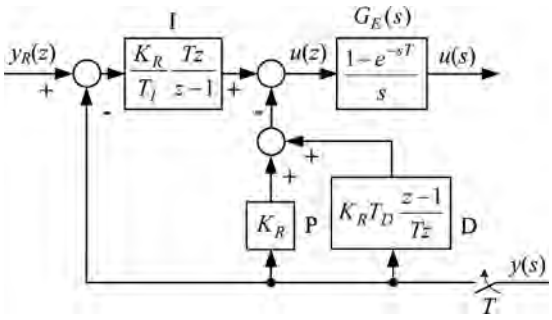

Fig. 2. Block diagram of discrete-time PID controller with zero-order-hold element at controller output.

the closed-loop system of any order l has a quasi-aperiodic step response characterized by an overshoot of approximately 6% (thus resembling a second-order system with damping ratio $\zeta=0.707$) and the approximate settling time of $1.8–2.1T_e$, as illustrated in Fig. 3a. This particular closed-loop tuning may be regarded as optimal in those cases where small overshoot and related well-damped behavior are critical, such as in controlled electrical drives and related servodrive control applications. By choosing larger T_e value, the control system robustness is improved and the noise sensitivity is decreased (i.e. bandwidth $\Omega_{BW}\sim 1/T_e$), but, in turn, a slower response and less efficient disturbance rejection are obtained. For a reduced-order controller with the number of free parameters equal to r, only the dominant characteristic ratios $D_2,\ldots, D_{r+1}$ should be set to desired values. In this case, however, the non-dominant characteristic ratios (corresponding to non-dominant high-frequency closed-loop poles) cannot be adjusted arbitrarily, so their effect to closed-loop damping should be analyzed separately. In general, the response damping is adjusted through varying the characteristic ratios D_2, D_3, … D_l, wherein the damping of dominant closed-loop dynamics (i.e. the dominant closed-loop poles damping ratio) is primarily influenced by the most dominant characteristic ratio D_2. By reducing the characteristic ratio D_2 to approximately 0.35 the fastest (boundary) aperiodic step response without overshoot is obtained. On the other hand, if D_2 is increased above 0.5 the closed-loop system response damping decreases (see Fig. 3b).

The PID controller ($r=3$) can arbitrarily adjust only the closed-loop characteristic ratios D_2, D_3 and D_4. Hence, the analytical expressions for PID controller proportional gain K_R, integral time constant T_I, and derivative time constant T_D are obtained by equating lower-order coefficients of the characteristic polynomial in (3) with the coefficients of the characteristic polynomial (4) up to s^4, which after some manipulation and rearranging yields the following relatively simple analytical expressions:

$$K_R=\frac{1}{K_p}\left(\frac{n(n-1)T_p^2}{2D_2^2D_3T_e^2}-1\right), \tag{5}$$

$$T_I=\left(1-\frac{2D_2^2D_3T_e^2}{n(n-1)T_p^2}\right)T_e, \tag{6}$$

$$T_D=D_2T_eT_pn\frac{(n-1)T_p-2D_2D_3T_e}{n(n-1)T_p^2-2D_2^2D_3T_e^2}, \tag{7}$$

with the closed-loop equivalent time constant T_e given as follows (valid for $n>2$):

$$T_e=\frac{(n-2)T_p}{3D_2D_3D_4} \tag{8}$$

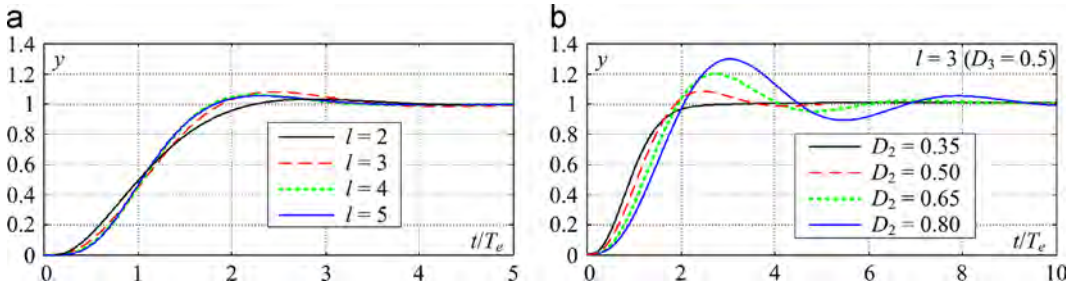

Fig. 3. Step response of prototype system tuned according to damping optimum (a) and illustration of closed-loop damping variation through dominant characteristic ratio D_2 (b).

Similarly, in the case of PI controller ($T_D=0$), only the closed-loop characteristic ratios D_2, D_3 can be tuned, so the design is based on the coefficients of the characteristic polynomial (4) up to s^3:

$$K_R=\frac{1}{K_p}\left(\frac{nT_p}{D_2T_e}-1\right), \tag{9}$$

$$T_I=\left(1-\frac{D_2T_e}{nT_p}\right)T_e, \tag{10}$$

while the equivalent time constant T_e is now given by (valid for $n>1$):

$$T_e=\frac{(n-1)T_p}{2D_2D_3} \tag{11}$$

The above expressions indicate that the PID controller parameters K_R, T_I and T_D are directly influenced by the dominant characteristic ratios D_2 and D_3, while the non-dominant characteristic ratio D_4 only affects the closed-loop equivalent time constant T_e. Similarly, the simpler PI controller tuning is directly affected by the most dominant characteristic ratio D_2, while the closed-loop equivalent time constant T_e directly depends on the less-dominant characteristic ratio D_3 value. Thus, it appears that the closed-loop response speed and dominant-mode damping tuning can be effectively decoupled, because the damping of the dominant closed-loop system modes is primarily determined by the choice of the most dominant characteristic ratio D_2, while the response speed primarily depends on the closed-loop equivalent time constant T_e.

It should be noted, however, that for the cases of first-order lag model ($n=1$) or a second-order model ($n=2$), the above expressions for PI and PID controller parameters (5)–(11) are characterized by a singularity. Namely, in those particular cases the PI and PID controllers may be considered as respective full-order controllers, which results in an arbitrary choice for the equivalent time constant T_e (see discussion above). For those particular cases, the expressions for controller parameters are listed in Table 1. Note, however, that a too small T_e choice would result in significant control efforts and controller output saturation during reference or disturbance response transients. Moreover, the closed-loop system noise sensitivity (i.e. bandwidth Ω_{BW}) is directly related to the T_e value ($\Omega_{BW}\sim 1/T_e$), so the closed-loop equivalent time constant should also have to be chosen such as to achieve favorable suppression of the measurement noise and related chattering effects in the controller output (manipulated variable) u.

Since PI and PID controller are of a relatively low order, they cannot arbitrarily set the higher, non-dominant characteristic ratios in the case of a high-order closed-loop system, so the effect of high-order closed-loop modes is analyzed herein in terms of damping optimum criterion and closed-loop system root-locus plots. By combining Eqs. (3) and (4), and using the expression (2) for the process parameters a_m, the higher-order characteristic ratios D_m (where $m>3$ for PI controller, and $m>4$ for PID controller) can be expressed by the following simple relation:

$$D_m=\frac{(n-m+1)(m-1)}{(n-m+2)m}=\left(1-\frac{1}{n-m+2}\right)\left(1-\frac{1}{m}\right). \tag{12}$$

These characteristic ratios should be close to 0.5 for higher-order characteristic ratios (i.e. higher m):

$$\lim_{m\to n}D_m=\frac{1}{2}\left(1-\frac{1}{n}\right), \tag{13}$$

which points out to well-damped nature of high-frequency modes.

Fig. 4 shows the root-locus plots of closed-loop systems with PI and PID controller (normalized with respect to the PTn model time constant T_p), for a wide range of process model orders n. The root-locus plots confirm that the higher-order closed-loop modes are indeed well-damped, i.e. the less-dominant closed-loop poles (corresponding to higher-frequency modes) are all characterized by damping ratio $\zeta\approx 0.707$.

Table 1
PI and PID controller parameters for first-order and second-order process model formulations.

Controller (process model order)	
PI ($n=1$)	PID ($n=2$)
$K_R=\frac{1}{K_p}\left(\frac{T_p}{D_2T_e}-1\right)$	$K_R=\frac{1}{K_p}\left(\frac{T_p^2}{D_3D_2^2T_e^2}-1\right)$
$T_I=T_e\left(1-\frac{D_2T_e}{T_p}\right)$	$T_I=T_e\left(1-\frac{D_3D_2^2T_e^2}{T_p^2}\right)$
–	$T_D=T_p\left(\frac{T_p}{D_3D_2T_e}-2\right)$

2.3. Discrete-time PID controller implementation

In the case when the PID controller is implemented as a discrete-time controller (Fig. 2), the design procedure can still be carried out in the continuous-time domain if the influence of the time-discretization (sampling) is adequately taken into account. The series connection of the sampler and the zero-order hold (ZOH):

$$G_{sE}(s)=\frac{1}{T}G_E(s)=\frac{1-e^{-sT}}{Ts}, \tag{14}$$

corresponds to a $T/2$ delay (T is the sampling time) cascaded to the process [41].

The time-differentiation effective delay $T/2$ of the PID controller derivative term $(z-1)/(Tz)$ [42] can be added to the $T/2$ time delay due to the sampler and time-discretization, thus resulting in the overall parasitic time delay $T_{par}=T$. This equivalent parasitic time delay can then be lumped with the process equivalent dead-time T_d (see e.g. [41]), obtained by the FOPDT model identification procedure described in Section 3.

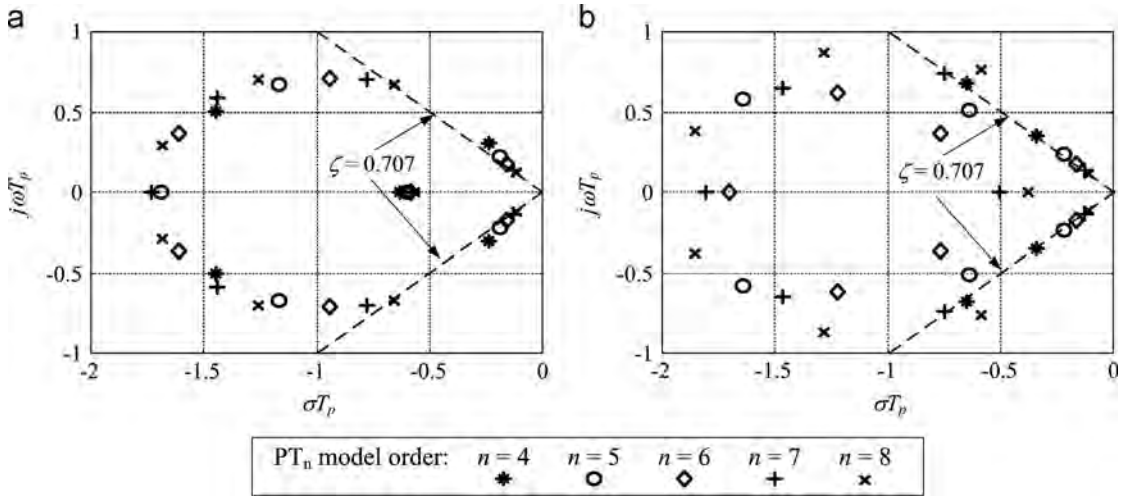

Fig. 4. Normalized root-locus plots of optimally-tuned closed loop-systems with PI controller (a) and PID controller (b) for different PTn process model orders.

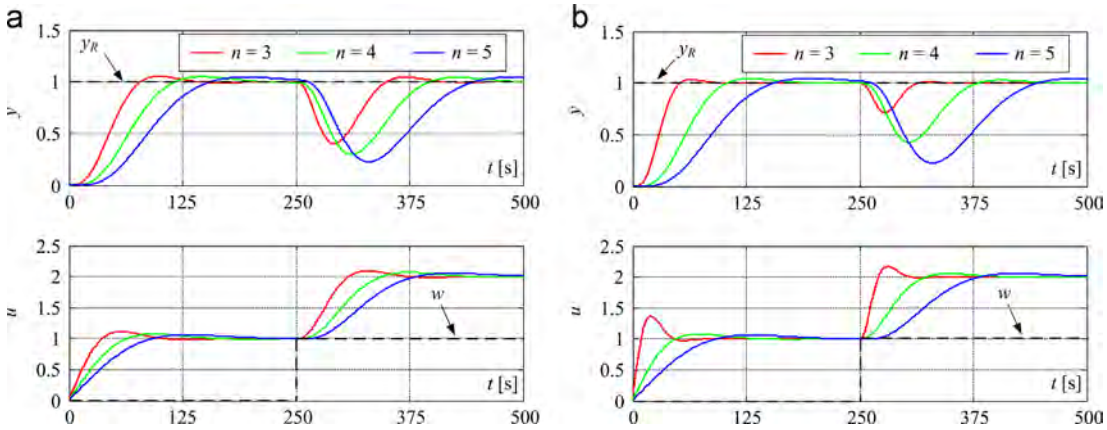

Fig. 5. Reference and disturbance step responses of control systems with PI controller (a) and PID controller (b) for different orders of PTn process model.

The sampling time choice (where possible) represents a trade-off between the controller performance and its computational burden and measurement noise issues. For processes with notable response pure delay, the sampling time T is typically chosen with respect to the equivalent process dead-time T_d and lag time constant T_a of the process step response (see Section 3) as follows [41]

$$T \approx \begin{cases} (0.35-1.2)T_d, & 0.1 \le T_d/T_a \le 1, \\ (0.22-0.35)T_d, & 1 \le T_d/T_a \le 10. \end{cases} \quad (15)$$

Note, however, that in the case of commercial PID controller modules (see e.g. [12]), or PLC control hardware configuration utilizing intelligent sensors (with internal signal processing features and typically fixed data transfer rate), the controller sampling rate may be pre-determined by the control hardware internal design. Therefore, in those cases the sampling time may not be regarded as the controller design parameter chosen relatively freely according to Eq. (15), but rather as a fixed parameter which needs to be taken into account during the controller design (tuning), as explained earlier.

2.4. Simulation verification of controller tuning

The properties of the proposed PI and PID controller tuning approach are illustrated in Figs. 5 and 6 by simulation results. Fig. 5 shows the comparative simulation responses of continuous-time closed-loop systems with PI and PID controllers tuned for a damping-wise conservative, quasi-aperiodic response ($D_2=D_3=D_4=0.5$) and PTn process models characterized by $K_p=1$, $T_p=10$ s and model orders in the range $n=3$–5. The results show that the proposed controller tuning with all dominant characteristic ratios set to 0.5 indeed results in well-damped control system responses with respect to both the reference y_R and input disturbance w step changes, characterized by approximately 6% response overshoot. As expected, the closed-loop equivalent time constant T_e, and, hence, the control system response time increases with the process order n (cf. Eqs. (8) and (11)). Note also that for low process model order $n=3$, the PID controller results in a much faster step reference response and notably improved disturbance rejection compared to PI controller, because in that particular case the PID controller design yields a notably smaller value of the closed-loop equivalent time constant ($T_e=26.7$ s) compared to PI controller ($T_e=40$ s). However, as the process model order increases, the aforementioned discrepancy becomes smaller, and the PID controller yields control system performance similar to simpler PI controller.

The closed-loop step responses in Fig. 6 illustrate the effects of varying the closed-loop equivalent time constant T_e according to Eqs. (8) and (11), wherein T_e adjustment reflects in the change of the less-dominant characteristic ratios (D_3 in the case of PI controller, and D_4 in the case of PID controller). If the closed-loop equivalent time constant T_e is increased above the design value according to (8) and (11), this results in a slower closed-loop response. As expected, by decreasing the closed-loop equivalent time constant T_e below these values, the response speed

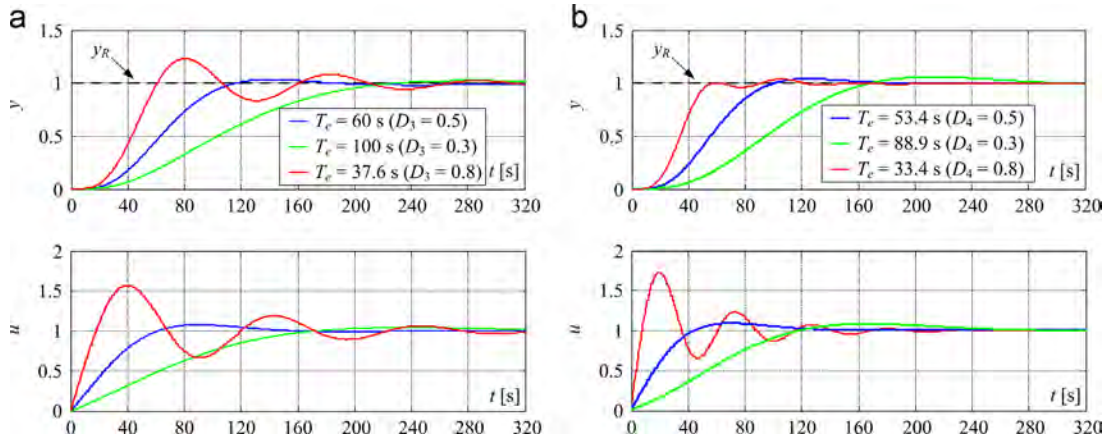

Fig. 6. Comparative control systems responses for PI controller (a) and PID controller (b) tuned with $D2=0.5$ and different values of closed-loop equivalent time constant T_e (PTn process model, $K_p=1$, $T_p=10$ s, $n=4$).

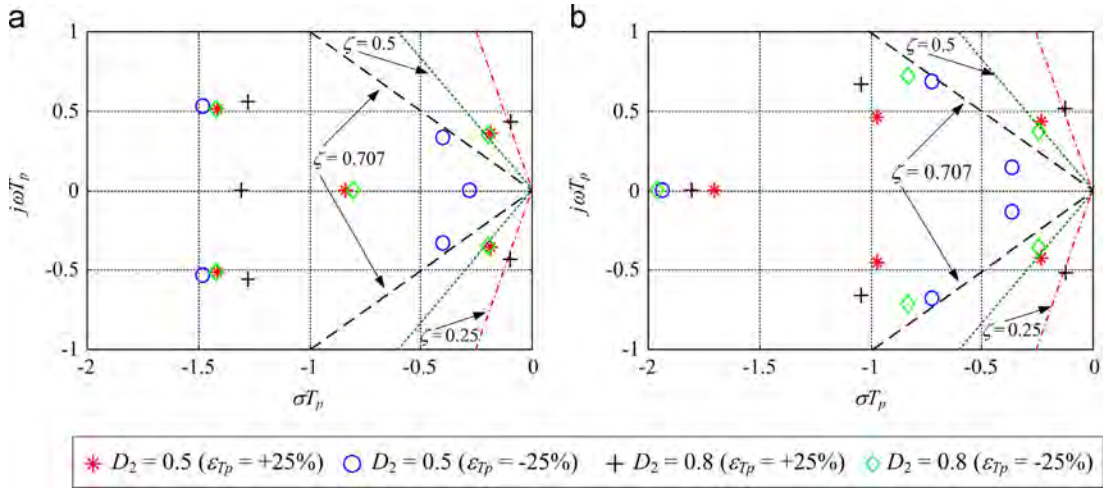

Fig. 7. Normalized root-locus plots of differently-tuned closed loop-systems with PI controller (a) and PID controller (b) for $\pm 25\%$ variations of PTn process model time constant T_p ($n=4$).

can indeed be increased. However, this corresponds to effective increase of less-dominant characteristic ratios (D_3 or D_4), and related lower damping of the less-dominant (higher-frequency) closed-loop modes.

2.5. Robustness analysis

The effects of PTn process model uncertainty to control system robustness (i.e. damping of dominant closed-loop modes) have been analyzed by means of root-locus plots and simulations for two choices of the most dominant characteristic ratio D_2 used in PI/PID controller design (with D_3, $D_4=0.5$), and a fourth-order PTn process model formulation. Note that the results of dominant mode damping analysis should generally be valid for a wide range of PTn model orders n, because the damping of higher-order modes is not affected by controller tuning or by the value of PTn model time constant T_p (see results in Fig. 4 and the related discussion in Section 2.2). The modeling uncertainty effects are examined for the case of relatively large $\pm 25\%$ variation of the PTn model time constant T_p, reflected through its relative error $\varepsilon_{Tp}=T_p/T_{pn}-1$ (where T_{pn} is the nominal PTn model time constant used in PI/PID controller design and T_p is the actual time constant value).

The normalized root locus plots in Fig. 7 show that for the case of PI and PID controller tuned for a damping-wise conservative behavior ($D_2=0.5$), the dominant conjugate-complex closed-loop pole pair for $\varepsilon_{TP}=-25\%$ ($T_p<T_{pn}$) is shifted towards the area of higher damping ($\zeta>0.707$), while in the case of T_p larger then nominal ($\varepsilon_{TP}=+25\%$), the aforementioned pole pair remains fairly well-damped ($\zeta\approx 0.5$). On the other hand, for the case of PI and PID controller tuned less-conservatively, i.e. with higher D_2 value ($D_2=0.8$) corresponding to weaker damping (and faster response), the dominant closed-loop poles are shifted towards the area of somewhat weaker damping ($0.5<\zeta<0.25$), which may still be acceptable for process control applications favoring fast response over closed-loop damping considerations [12].

The root-locus results in Fig. 7 are also corroborated by the closed-loop system simulation results shown in Fig. 8 (with the time responses also normalized with respect to time constant T_p). The results show that for the case of damping-wise conservative tuning ($D_2=0.5$) the closed-loop responses are indeed rather well-damped, with notably slower (aperiodic) response without overshoot occurring for the case of time constant T_p smaller nominal ($\varepsilon_{Tp}=-25\%$). By tuning the PI or PID controller less conservatively ($D_2=0.8$), faster closed-loop responses can be obtained, but this is indeed paid for by somewhat more oscillatory reference step response.

Based on the above results, the proposed method apparently ensures a favorable level of closed-loop system robustness in the presence of rather large process model uncertainty even for the

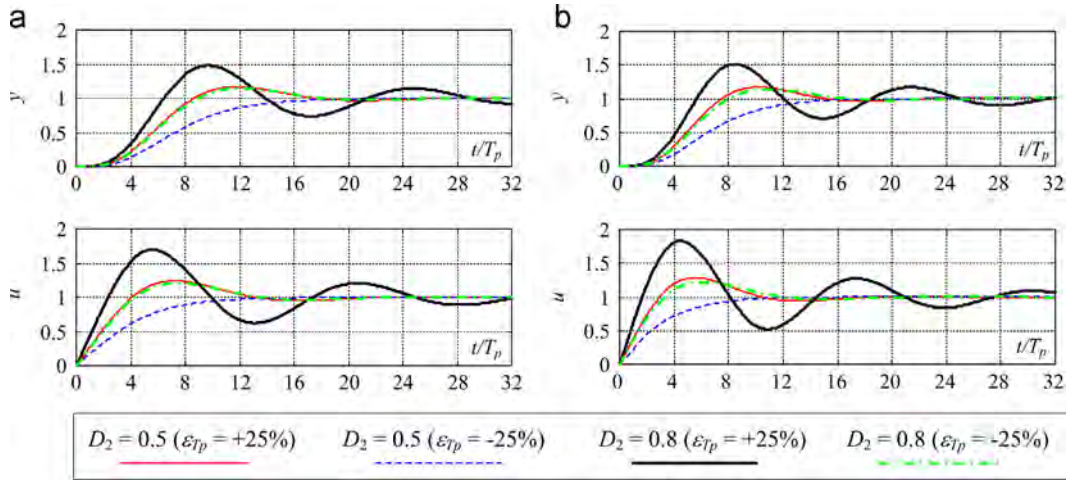

Fig. 8. Normalized simulation responses of differently-tuned closed loop-systems with PI controller (a) and PID controller (b) for ±25% variations of PTn process model time constant T_p ($n=4$).

case of damping-wise less-conservative controller tuning choice. Still, the choice of the main PI/PID controller tuning parameter (i.e. characteristic ratio D_2) is obviously a trade-off between the closed-loop response speed performance, and the prescribed (desired) lower bound of the dominant closed-loop modes damping ratio.

3. Process model identification

This section presents the estimation of aperiodic process model parameters based on the process step response integration and identification of equivalent FOPDT process model (the so-called area method). The proposed process model identification approach is compared to the traditional flexion tangent method of estimation of FOPDT and PTn process model parameters, and is used as a basis for a PID controller auto-tuning algorithm.

3.1. Step response flexion tangent approach

Traditionally, processes characterized by aperiodic step response and notable initial delay (equivalent dead-time) are modeled by using the equivalent first-order plus dead-time (FOPDT) process model:

$$G_p(s)=\frac{K_p e^{-sT_d}}{1+T_a s} \tag{16}$$

where the equivalent dead-time T_d and the time constant T_a of the first-order lag term are typically determined by the so-called flexion-tangent approach [31], as illustrated in Fig. 9. In order to obtain a more convenient dead-time-free process model (suitable for PI/PID controller tuning described in Section 2), the FOPDT process model can be directly related to the more accurate PTn process model (1), characterized by the same response slope (time-derivative) at the flexion point (the so-called Strejc method [30]). The relationships between the FOPDT model and PTn process model parameters are given by

$$\frac{T_d}{T_a}=e^{(1-n)}\left[\frac{(n-1)^n}{(n-1)!}+\sum_{m=0}^{n-1}\frac{(n-1)^m}{m!}\right]-1, \tag{17}$$

$$\frac{T_p}{T_a}=\frac{(n-1)^{n-1}}{(n-1)!}e^{(1-n)}, \tag{18}$$

with the results of numerical evaluation of above equations for $n=$ 2–10 shown in Table 2.

Note, however, that the accuracy of thus obtained FOPDT model is favorable only over the equivalent dead-time interval Td and in the vicinity of the process response flexion point, while the later part of the process transient response is captured less accurately (see Fig. 9).

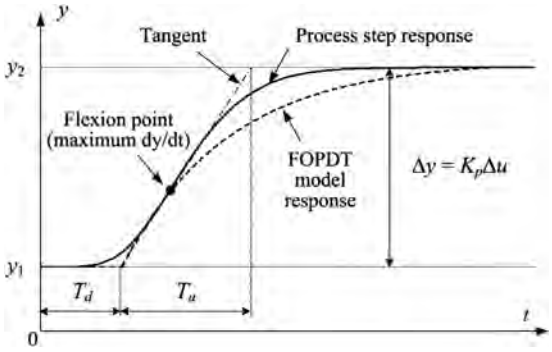

Fig. 9. Illustration of identification of FOPDT model based on the step response flexion tangent approach.

3.2. FOPDT process model identification based on step response integration

Since the above flexion tangent identification method may be sensitive to process measurement noise (when finding the response time-derivative maximum point), the FOPDT model may instead be identified based on the step response time-integral (area) method [43], shown in Fig. 10. In this approach, the process step response time integral is related to the FOPDT model response in the following manner:

$$I_1=\int_0^{T_{fin}}(y(t)-y_1)dt\approx\int_0^{T_{fin}}(y_2-y_1)[1-e^{-(t-T_d)/T_a}]dt$$
$$=(y_2-y_1)\left[T_{fin}-T_d-T_a+T_a e^{-(T_{fin}-T_d)/T_a}\right], \tag{19}$$

If the identification interval T_{fin} is larger than $5T_a+T_d$ (the steady-state condition), the exponential term on the rightmost side of Eq. (19) becomes negligible (i.e. it is less than 0.01), and the following relationship is valid:

$$T_a=T_{fin}-T_d-\frac{I_1}{y_2-y_1}, \tag{20}$$

The process model equivalent dead-time T_d can be determined by means of a simple threshold crossing logic, as illustrated in Fig. 10, while the process model gain K_p is estimated based on the

Table 2
Relationships between FOPDT model and equivalent PTn model according to flexion-tangent approach.

n	2	3	4	5	6	7	8	9	10
T_d/T_a	0.1036	0.2179	0.3195	0.4098	0.4926	0.5714	0.6410	0.7092	0.7752
T_p/T_a	0.3679	0.2707	0.2240	0.1954	0.1755	0.1606	0.1490	0.1396	0.1318

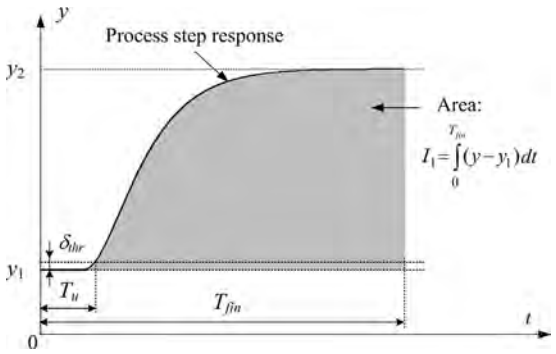

Fig. 10. Illustration of process response integration (area) method for identification of FOPDT model.

process steady-states y_2 and y_1 and the input step magnitude Δu as $K_p=(y_2-y_1)/\Delta u$ (see Fig. 9).

In practical applications, the above FOPDT process model identification procedure (implemented as a discrete-time algorithm) would also need to include the following features:

- *Process output averaging* (low-pass filtering) required to correctly estimate the process initial state y_1 and the step response steady-state y_2 in the presence of process output measurement noise. This can be facilitated by using a simple first-order low-pass term (filter):

$$y_f(kT_s)=a_f y_f(kT_s-T_s)+(1-a_f)y(kT_s), \tag{21}$$

  where T_s is the process response sampling time, and the discrete-time filter coefficient a_f is related to the filter equivalent time constant T_f as $a_f=\exp(-T_s/T_f)$. The same filtered output signal can conveniently be used for the detection of process response equivalent dead-time. Note that in that case the dead-time value T_{df} obtained from the filtered process output should be adjusted with respect to the low-pass filter equivalent delay (corresponding to filter time constant T_f):

$$T_d=T_{df}-T_f. \tag{22}$$

  Finally, the low-pass filter can also be used to detect the process response settling after the step transient by monitoring the time-difference of the low-pass filtered process output $\Delta y_f(kT_s)=y_f(kT_s)-y_f(kT_s-T_s)$, where the steady-state could be detected by simple threshold logic (i.e. the settling would be indicated by $|\Delta y_f(kT_s)|\le\Delta y_{thr}$).
- *Estimation of process output noise RMS* in order to find a proper threshold value δ_{thr} for the detection of process response equivalent dead-time T_d.
- *Process response numerical integration*, wherein a relatively simple trapezoidal integration formula (Tustin integration method) can be used to approximate expression (19):

$$I_1(kT_s)=I_1(kT_s-T_s)+\frac{T_s}{2}[y(kT_s)+y(kT_s-T_s)-2y_1]. \tag{23}$$

Note that the accuracy of the FOPDT process model parameters estimation (primarily reflected through the accuracy of lag constant T_a estimation) is directly related to the error bound Δ_I of the trapezoidal integration formula given by [44]:

$$|\Delta_I|\le\frac{T_{fin}T_s^2}{12}\left|\max_{t\in[0,T_{fin}]}\ddot{y}(t)\right|, \tag{24}$$

which for the case of FOPDT model (16) step response can be rewritten as

$$|\Delta_I|\le\frac{T_{fin}T_s^2}{12\,T_a^2}|y_2-y_1|. \tag{25}$$

The above result, in combination with Eq. (20) gives the following estimate of T_a absolute and relative error upper bounds, respectively:

$$\left|\Delta\hat{T}_a\right|\le\frac{T_{fin}T_s^2}{12\,T_a^2}, \tag{26}$$

$$\frac{|\Delta\hat{T}_a|}{T_a}\le\frac{1}{12}\frac{T_{fin}T_s^2}{T_a\,T_a^2}. \tag{27}$$

Since the T_a estimation error upper bound decreases with the T_s vs. T_a ratio squared, the estimation accuracy should not be an issue provided that the process response is notably slower (T_a value much larger) than the integration step size T_s, and that the response integration interval T_{fin} is also bounded with respect to the actual T_a value (which is ensured by the utilization of the process response steady-state detection logic).

3.3. Evaluation of equivalent PTn model parameters

However, the FOPDT model dead-time T_d and the lag time constant T_a obtained by the above identification procedure cannot be used to directly calculate the PTn model parameters according to (17) and (18), because the flexion tangent slope equivalence no longer holds. In order to find the parameters of the dead-time-free equivalent higher-order process model, the pure delay can be approximated by its Taylor expansion [43]:

$$e^{-sT_d}=\frac{1}{e^{sT_d}}\approx\frac{1}{1+T_ds+(T_d^2s^2/2)+(T_d^3s^3/6)+\cdots}, \tag{28}$$

which results in the following approximation of the FOPDT model (16):

$$G_p(s)=\frac{K_p}{1+(T_d+T_a)s+((T_d/2)+T_a)T_ds^2+((T_d/6)+(T_a/2))T_d^2s^3+((T_d/24)+(T_a/6))T_d^3s^4+\cdots}. \tag{29}$$

The above dead-time-free model can be related to the compact PTn model (1) conveniently used in PID controller design by equating the first three (dominant) coefficients of the PTn model characteristic polynomial (1) with those of the process model approximation (29). After some manipulations and rearranging, the following expression for the PTn model order n is obtained (which is then rounded to the nearest integer value):

$$n=\frac{2}{1-T_d(T_d+3T_a)/((T_d+T_a)(T_d+2T_a))}. \tag{30}$$

Similarly, the relationship between the PTn model time constant T_p and the FOPDT model dead-time T_d and lag time constant

T_a is obtained in the following form (valid for $n>2$):

$$T_p = \sqrt{\frac{T_d(T_d+T_a)(T_d+3T_a)}{n(n-2)(T_d+2T_a)}} \tag{31}$$

In the special case when the process equivalent dead-time T_d is rather small, $n=2$ may be obtained (after rounding). In that case, the time constant T_p should be calculated by using a simpler expression:

$$T_p = \frac{T_d(T_d+2T_a)}{(n-1)(T_d+T_a)}. \tag{32}$$

which is obtained by equating lower-order coefficients of the characteristic polynomials (1) and (29).

In the case of discrete-time (digital) controller (Section 2.3), the equivalent dead-time T_d should also include effect of time-discretization (sampling with controller sampling time T), zero-order-hold (ZOH) element and time-differentiation (PID controller only) in order to facilitate straightforward continuous-time domain controller design (Section 2). This is done by lumping the parasitic time delay T_{par} to the FOPDT model equivalent time constant T_d (with $T_{par}=T/2$ for PI controller, and $T_{par}=T$ for PID controller)

$$T_d^* = T_d + T_{par}, \tag{33}$$

and using the modified equivalent dead-time T_d^* instead of the estimated equivalent dead-time T_d for the evaluation of parameters of the controller design-oriented PTn process model (Eqs. (30)–(32)).

4. Simulation results

4.1. Process model identification results

The effectiveness of the proposed PTn model identification procedure is first illustrated through comparison with the traditional flexion-tangent method for the case of process model (taken from [41]) comprising aperiodic dynamics, dead-time and a relatively non-emphasized transfer function zero:

$$G_p(s) = \frac{y(s)}{u(s)} = \frac{(1+T_4 s)e^{-T_t s}}{(1+T_1 s)(1+T_2 s)(1+T_3 s)}, \tag{34}$$

with the following values of time constants $T_1=3$ s, $T_2=7$ s, $T_3=10$ s, $T_4=2$ s, and the dead-time T_t taking a relatively large range of values $T_t=\{4\text{ s}, 8\text{ s}, 12\text{ s}, 16\text{ s}\}$ for the sake of detailed simulation analysis.

Fig. 11 shows the comparative results of FOPDT and PTn process model identification with the choice of identification sampling time $T_s=0.1$ s. The numerical values of the estimated parameters of the FOPDT and PTn process models, are given in Table 3, along with the and the model prediction RMS error:

$$RMS_e = \sqrt{\frac{1}{N}\sum_{k=0}^{N-1}(y(k)-\hat{y}(k))^2}, \tag{35}$$

where $y(k)$ is the output of the process model (34), and $\hat{y}(k)$ is the predicted output of the identified FOPDT or PTn process model.

The results in Fig. 11a show that the proposed area-based FOPDT model identification procedure results in a much better fit of the process model response compared to the case of flexion-tangent

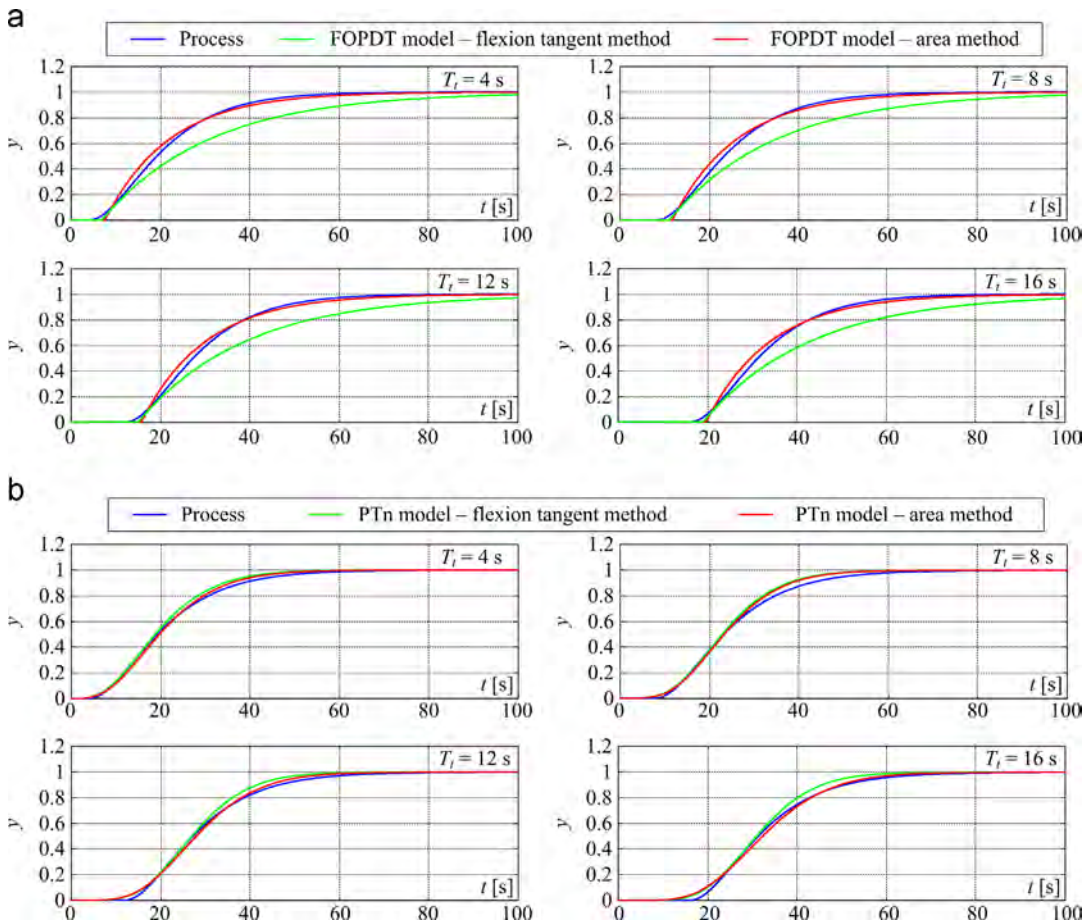

Fig. 11. Comparative results of identification of FOPDT model (a) and PTn model (b) by means of flexion tangent and area method for different values of pure delay in model (34).

Table 3
Comparative parameters of FOPDT and PTn models obtained by flexion tangent and area method, and related model RMS prediction errors.

Pure delay	Method	FOPDT model			PTn model		
		T_d [s]	T_a [s]	RMS error	n	T_p [s]	RMS error
$T_t=4$ s	Flexion tangent	6.94	24.04	32.05×10^{-4}	4	5.13	6.87×10^{-4}
	Area	7.50	14.48	7.27×10^{-4}	4	5.37	4.54×10^{-4}
$T_t=8$ s	Flexion tangent	10.94	24.03	32.07×10^{-4}	6	4.05	7.85×10^{-4}
	Area	11.50	14.47	7.29×10^{-4}	5	5.20	4.59×10^{-4}
$T_t=12$ s	Flexion tangent	14.94	24.04	32.02×10^{-4}	8	3.52	8.13×10^{-4}
	Area	15.50	14.45	7.32×10^{-4}	6	5.06	6.61×10^{-4}
$T_t=16$ s	Flexion tangent	18.94	24.02	31.99×10^{-4}	10	3.20	8.64×10^{-4}
	Area	19.50	14.43	7.35×10^{-4}	8	4.23	5.92×10^{-4}

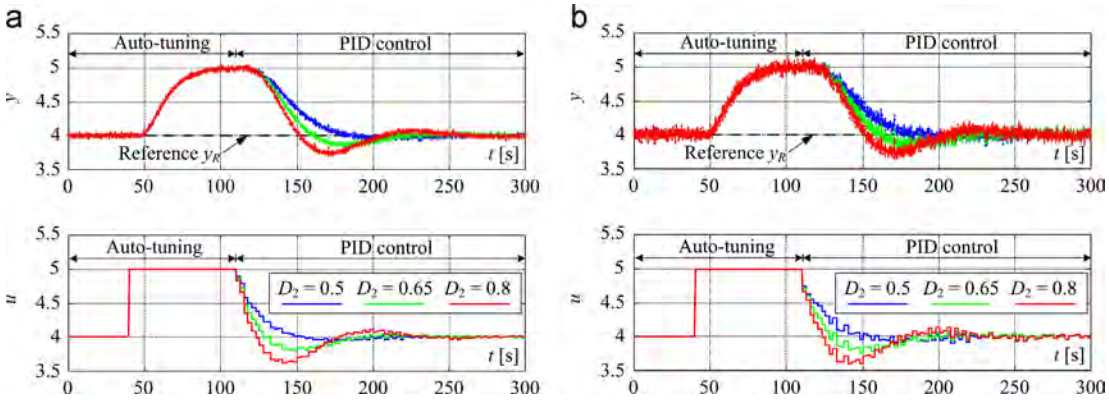

Fig. 12. Simulation results of auto-tuning PID control in presence of measurement noise for identification integration step $T_s=0.1$ s much smaller than controller sampling time T (process model (34) with $T_t=8$ s): noise RMS=0.02 (a), and noise RMS=0.05 (b).

method, which gives good approximation of the process model dynamics only in the vicinity of the step response flexion point. Namely, according to Table 3, both identification methods yield similar values of the equivalent FOPDT model dead time, but the flexion-tangent method overestimates the equivalent lag time constant T_a by approximately 65%. This results in much slower settling of the flexion tangent-based FOPDT model response (cf. Fig. 11), and significantly larger model RMS prediction errors compared to the FOPDT model obtained by area-based identification method. The responses of the related PTn process models are shown in Fig. 11b. These responses, along with the prediction error RMS data in Table 3, also point out to a notably better process step response fit obtained by the area method, both during the transient phase and in the response settling stage.

4.2. Auto-tuner simulation verification

The proposed PTn process model identification procedure is also tested within the framework of PID auto-tuning by means of simulations. In order to test the robustness of the process model identification and the related PID controller auto-tuning algorithm, a Gaussian noise source has been added to the process output. This mainly concerns the practical aspects of the process PTn model identification (see Section 3.2): the choice of detection thresholds δ_{thr} and Δy_{thr}, and the bandwidth (time constant T_f) of the process response low-pass filter. The low-pass filter time constant T_f is chosen such as to facilitate favorable noise attenuation (averaging) properties. The threshold values δ_{thr} and Δy_{thr} are adjusted with respect to the steady-state noise RMS value (RMS_{ss}) according to (35) with replaced with the process steady-state response y_{ss} (obtained from the process response low-pass filter (21)). In order to ensure robust detection of both the equivalent dead-time T_d and the response settling, the choices $\delta_{thr}=1.6{\cdot}RMS_{ss}$ and $\Delta y_{thr}=0.05\cdot RMS_e$ are used herein. Two process model identification scenarios have been considered:

Table 4
Results of process model identification during PID controller auto-tuning simulation tests for different measurement noise RMS values.

Noise RMS	T_a [s]	T_d [s]	T [s]	T_d^* [s]	n	T_p [s]	K_p
0.02	14.27	11.3	4.0	15.3	6	4.98	0.990
0.05	14.04	12.0	4.2	16.2	7	4.30	0.993

(i) identification with the same identification sampling time (integration step size) $T_s=0.1$ s as in the noise-free case in Fig. 11, corresponding to controller with flexible sampling time choice, and
(ii) identification with larger sampling times in order to illustrate the effectiveness of the proposed identification algorithm for the case of controller with fixed sampling rate (i.e. $T_s=T$).

Fig. 12 shows the comparative responses of the auto-tuning PID controller with identification sampling time $T_s=0.1$ s applied to the process model (34) with process model dead-time $T_t=8$ s, and for the cases of process noise RMS set to 2% and 5% of the process output step response magnitude. In the initial phase of auto-tuning ($t<40$ s), the process initial state and the noise RMS are estimated, which is then followed by the step response-based process model identification, and final closed-loop verification of the PID controller tuned with different values of the dominant

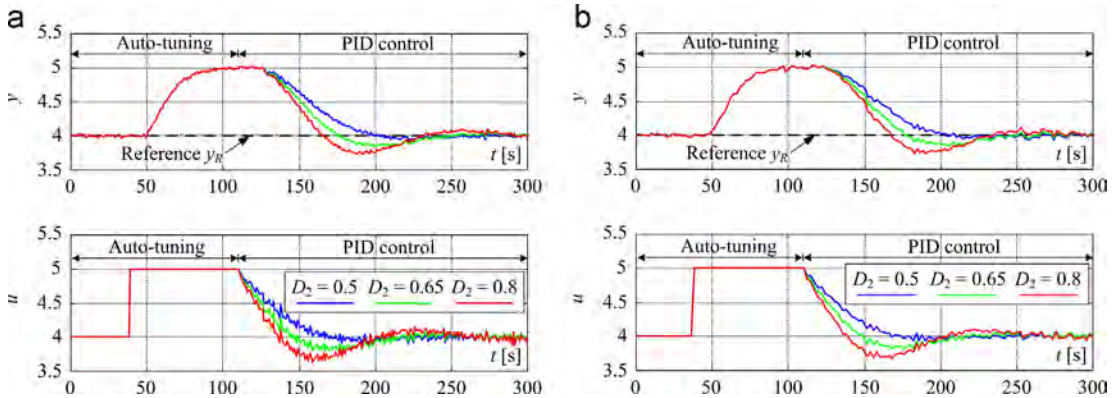

Fig. 13. Simulation results of auto-tuning PID control for fixed integration step T_s equal to controller sampling time T (process model (34) with T_t=8 s) with noise RMS=0.02: T_s=1 s (a), and T_s=2 s (b).

characteristic ratio D_2. The identification results summarized in Table 4 indicate that the proposed area-based FOPDT model identification procedure is fairly robust even in the presence of relatively large-magnitude process noise, and results in highly-consistent estimation of FOPDT and PTn process model parameters. Note, however, that the choice of discrete-time PID controller sampling time[2] T according to recommendation (15) results in a slower controller sampling rate (see Table 4), and approximately 30% larger "lumped" dead-time parameter T_d^* used for the evaluation of the PTn process model parameters. After the auto tuning phase is finished, the PID controller is turned on, and a constant reference is applied to the closed-loop system. The auto-tuned PID controllers are characterized by different levels of closed loop damping depending on the choice of the dominant characteristic ratios D_2 (with D_3=D_4=0.5). As expected, a well-damped (quasi-aperiodic) reference step response is obtained when D_2 is set to 0.5. As the dominant characteristic ratio D_2 is increased above 0.5, the closed-loop response time and damping are in turn decreased in accordance with the damping optimum criterion tuning properties (cf. Fig. 3b). In all cases, the controller output (manipulated variable u) is characterized by a relatively small magnitude of noise due to controller bandwidth being effectively limited due to a relatively large equivalent closed-loop time constant T_e.

The auto-tuner simulation results for the case of much larger identification sampling times and auto-tuner/controller fixed sampling rate (T_s=T) are shown in Fig. 13. The presented results indicate that the proposed identification approach works well even for relatively large sampling times T_s (comparable to process model (34) lag time constants), and ultimately results in anticipated closed-loop behavior for the particular D_2 tuning parameter choices (cf. results in Fig. 12).

5. Conclusion

The paper has presented a novel analytical method of PID controller tuning based on the n-th order aperiodic process model description (PTn model) and the utilization of damping optimum criterion, which facilitates a rather straightforward adjustment of both closed-loop system damping and response speed, and whose main features have been verified by means of simulations. The effect of modeling errors has been examined by root locus plots and simulation analysis, which have shown that the proposed tuning method can facilitate fairly robust closed-loop behavior in the presence of relatively large process model variations (i.e. PTn process model time constant).

In order to find the parameters of the controller design-oriented PTn process model, a relatively computationally-simple auto-tuning algorithm based on process model step response time integral has been developed and tested. The auto-tuning algorithm finds the parameters of the simplified first-order plus dead-time (FOPDT) process model, which is then related to the dead-time-free PTn process model used in PID controller design by using a higher-order Taylor expansion of the process equivalent dead-time term.

The proposed step response-based PTn process model identification has been verified on a prototype process model comprising both the aperiodic (lag) dynamics and emphasized dead-time effect, and it has resulted in a consistent estimation of key parameters of the equivalent PTn model for a wide range of the process dead-time parameter values, while also achieving notably improved model prediction accuracy compared to the traditional flexion-tangent identification approach. The overall auto-tuning PID controller has also been verified by means of simulations. The PTn model identification procedure has shown favorable robustness in the presence of emphasized process measurement noise and for a wide range of sampling time choices. The resulting automatically-tuned PID controllers have yielded expected (favorable) closed-loop system behavior, wherein the closed-loop system dominant mode damping is easily tuned by means of the damping optimum tuning method.

Future work may be directed towards the development of auto-tuning procedures for other process model structures and related refinement of the damping optimum criterion-based PID controller tuning.

[2] In order to avoid noise aliasing issues in the case of relatively large controller sampling time T choice, the high-sampling-rate process output (T_s=0.1 s) is averaged within the controller sampling time window (with the width W=T/T_s), thus substituting for the anti-aliasing low-pass filter of the process output signal.

Acknowledgment

The first author would like to express his appreciation to Prof. Joško Deur from the Faculty of Mechanical Engineering and Naval Architecture, University of Zagreb for his insights and helpful discussions regarding the damping optimum criterion.

References

[1] Bonivento C, Castaldi P, Mirotta D. Predictive control vs. PID control of an industrial heat exchanger. In: CD ROM Proceedings of 9th Mediterranean conference on control and automation (MED 2001), Dubrovnik, Croatia; 2001.
[2] Al-Dawery SK, Alrahawi AM, Al-Zobai KM. Dynamic modeling and control of plate heat exchanger. International Journal of Heat and Mass Transfer 2012;55 (23–24) (6873–5880).

[3] Åström KJ, Hägglund T. The future of PID control. Control Engineering Practice 2001;9(11):1163–75.
[4] Panda RC, Yu C-C, Huang H-P. PID tuning rules for SOPDT systems: review and some new results. ISA Transactions 2004;43(2):283–95.
[5] Åström KJ, Hägglund T. Revisiting the Ziegler–Nichols step response method for PID control. Journal of Process Control 2004;14(6):635–50.
[6] Leva A, Negro S, Papadopoulos AV. PI/PID autotuning with contextual model parametrisation. Journal of Process Control 2010;20(4):452–63.
[7] Li Y, Ang K-H, Chong G. Patents, software and hardware for PID control. IEEE Control Systems Magazine 2006;26(1):42–54.
[8] Ang K-H, Chong G, Li Y. PID control system analysis, design and technology. IEEE Transactions on Control Systems Technology 2005;13(4):559–76.
[9] Åström KJ, Hägglund T. Revisiting the Ziegler–Nichols step response method for PID control. Journal of Process Control 2004;14(6):635–50.
[10] Dey C, Mudi RK. An improved auto-tuning scheme for PID controllers. ISA Transactions 2009;48(4):396–409.
[11] Hagglund T, Åström KJ. Automatic tuning of PID controllers. In: Levine WS, editor. The control handbook. Boca Raton, FL, USA: CRC Press; 2000 [chapter 52].
[12] Åström KJ, Hägglund T. PID controllers: theory, design and tuning. 2nd ed.. Research Triangle Park, Durham, NC, USA: Instrument Society of America; 1995.
[13] Wang Q-G, Fung H-W, Zhang Y. PID tuning with exact gain and phase margins. ISA Transactions 1999;38(3):243–9.
[14] Atherton DP. Relay autotuning: a use of old ideas in a new setting. Transactions of the Institute of Measurement and Control 2000;22(1):103–22.
[15] Preitl S, Precup R-E. An extension of tuning relations after symmetrical optimum method for PI and PID controllers. Automatica 1999;35(10):1731–6.
[16] Lui T, Gao F. Relay-based autotuning of pid controller for improved load disturbance rejection. In: Proceedings of the 17th IFAC world congress, Seoul, South Korea; July 2008. p. 10933–38.
[17] Carnevale C, Piazzi A, Visioli A. A methodology for integrated system identification, PID controller tuning and noncausal feedforward control design. In: Proceedings of the 17th IFAC world congress, Seoul, South Korea; July 2008. p. 13324–29.
[18] Karimi A, Garcia D, Longchamp R. PID controller tuning using bode's integrals. IEEE Transactions on Control System Technology 2003;11(6):812–21.
[19] Padhy PK, Majhi S. Improved automatic tuning of PID controller for stable processes. ISA Transactions 2009;48(4):423–7.
[20] Hang CC, Åström KJ, Wang QG. Relay feedback auto-tuning of process controllers – a tutorial review. Journal of Process Control 2002;12(1):143–62.
[21] Wang Q-G, Zhang Y. Robust identification of continuous systems with dead-time from step response. Automatica 2001;37(3):377–90.
[22] Vrančić D, Peng Y, Strmčnik S. A new PID controller tuning method based on multiple integrations. Control Engineering Practice 1999;7(5):623–33.
[23] Vrančić D, Strmčnik S, Juričić Đ. A magnitude optimum multiple integration tuning method for filtered PID controller. Automatica 2001;37(9):1473–9.
[24] Vrančić D, Strmčnik S, Kocijan J, de Moura Oliveira PB. Improving disturbance rejection of PID controllers by means of the magnitude optimum method. ISA Transactions 2010;49(1):47–56.
[25] Villanova R. IMC based robust PID design: tuning guidelines and automatic tuning. Journal of Process Control 2008;18(1):61–70.
[26] Leva A. Comparative study of model-based PI(D) autotuning methods. In: Proceedings of the 2007 American control conference (ACC 2007), New York, USA; July 2007. p. 5796–801.
[27] Garpinger O, Hägglund T. A software tool for robust PID design. In: Proceedings of the 17th IFAC world congress, Seoul, South Korea; July 2008. p. 6416–21.
[28] Bi Q, Cai W-B, Wang Q-G, Hang C-C, Lee E-L, Sun Y, et al. Advanced controller auto-tuning and its application in HVAC systems. Control Engineering Practice 2000;8(6):633–44.
[29] Thomson M, Cassidy PG, Sandoz DJ. Automatic tuning of PID controllers using a combined time- and frequency-domain method. Transaction of the Institute of Measurement and Control 1989;11(1):40–7.
[30] Unbehauen H, Rao GP. Identification of continuous systems, North Holland; 1987 [chapter 4].
[31] Mikleš J, Fikar M. Process modelling, identification and control. Berlin-Heidelberg, Germany: Springer-Verlag; 2007 [chapter 6].
[32] Preuss HP. PTn-modell-identifikation im adaptiven PID-Regelkreis. Automatisierungstechnik 1990;38(9):337–43.
[33] Umland JW, Safiuddin M. Magnitude and symmetric optimum criterion for the design of linear control systems: what is it and how does it compare with the others. IEEE Transactions on Industry Applications 1990;26(3):489–97.
[34] Naslin P. Essentials of optimal control. London, UK: Iliffe Books; 1968 [chapter 2].
[35] Zäh M, Brandeburg G. Das erweiterte Dämpfungsoptimum. Automatisierungstechnik 1987;35(7):275–83.
[36] Deur J, Perić N, Stajić D. Design of reduced-order feedforward controller. In: Proceedings of the UKACC international conference on CONTROL'98, Swansea, UK; 1998. p. 207–12.
[37] Åström KJ, Wittenmark B. Computer controlled systems – theory and design. 3rd ed.. New Jersey, USA: Prentice Hall; 1997 [chapter 8].
[38] Schmidt C, Heinzl J, Brandenburg G. Control approaches for high-precision machine tools with air bearings. IEEE Transactions on Industrial Electronics 1999;46(5):979–89.
[39] Schröder D. ElektrischeAntriebe – Regelung von Antriebssystemen. 3rd ed. Berlin, Germany: Springer-Verlag; 2007 [chapter 19].
[40] Pavković D, Deur J, Lisac A. A torque estimator-based control strategy for oil-well drill-string torsional vibrations active damping including an auto-tuning algorithm. Control Engineering Practice 2011;19(8):836–50.
[41] Isermann R. Digital control systems, vol. 1. Berlin: Springer-Verlag; 1989 [chapter 5].
[42] Saito K, Kamiyama K, Ohmae T, Matsuda T, Microprocessor-Controlled Speed A. Regulator with instantaneous speed estimation for motor drives. IEEE Transactions on Industrial Electronics 1988;35(1):95–9.
[43] Normey-Rico JE, Camacho EF. Control of dead-time processes. London, UK: Springer-Verlag; 2007 [chapters 2 and 3].
[44] Kreyszig E. Advanced engineering mathematics. 8th ed. New York, USA: John Wiley & Sons; 1999 [chapter 17].